High Pressure Phase of Biphenyl at Room Temperature: A Monte Carlo Study

N. Arul Murugan,* Prakash Chandra Jha, S. Yashonath, and S. Ramasesha

Solid State and Structural Chemistry Unit, Indian Institute of Science, Bangalore-560012, India

Received: November 14, 2003; In Final Form: January 16, 2004

A new pressure-induced solid phase of biphenyl is reported at room temperature. Isothermal−isobaric ensemble variable shape simulation cell Monte Carlo calculations are reported on biphenyl at 300 K as a function of pressure between 0 and 4 GPa. The potential proposed by Williams for intermolecular and Benkert−Heine−Simmons (BHS) for intramolecular interactions have been employed. Different properties indicating changes in the crystal structure, molecular structure, distributions of inter- and intramolecular energy are reported as a function of pressure. With increase in pressure beyond 0.8 GPa, the dihedral angle distribution undergoes a change from a bimodal to an unimodal distribution. The changes in IR and Raman spectra across the transition computed from ab initio calculations are in agreement with the experimental measurements. It is shown that at pressures larger than 0.8 GPa, competition between intermolecular interactions with intramolecular terms viz., conjugation energy and the ortho−ortho repulsion favors a planar biphenyl due to better packing and consequently a predominant intermolecular term. The exact value of the transition pressure will depend on the accuracy of the inter- and intramolecular potentials employed here.

1. Introduction

Biphenyl exhibits a rich variety of phases with an increase in temperature.[1−3] Each of these phases is characterized by a different value of the dihedral angle between the two phenyl rings. In the gas phase, electron diffraction studies[4,5] suggest that the average dihedral angle is 44.4° ± 1.2°. Resonance associated with the aromatic rings gives rise to partial double bond character of the C−C bond bridging the phenyl rings. This leads to a shorter bond length of 1.5073 Å and favors a planar arrangement of the rings ($\phi = 0°$). In contrast, ortho−ortho repulsion between ortho hydrogens of the two rings favors a nonplanar arrangement. At lower temperatures, in the liquid phase or in solutions, the dihedral angle reduces significantly to 18−20°.[6,7] On further cooling, the liquid undergoes a transition to the solid phase. The average dihedral angle measured by X-ray diffraction is close to zero. Spectroscopic and other measurements suggest that the most probable dihedral angle is not zero; the phenyl rings are equally populated in the two minima of a double well potential.[8] At very low temperatures (<40 K) biphenyl exists in a conformation in which the average dihedral angle is about 10° (space group P_a).[2] Detailed studies have been carried out on biphenyl using a number of experimental methods such as electronic absorption and emission,[9] neutron scattering,[10] X-ray scattering,[3] Brillouin scattering,[11] nuclear magnetic resonance,[12] and Raman scattering methods.[13−15]

Ab initio calculations using CASSCF/DZP with a basis set of 4s3p1d/2s1p obtain a twist angle of 44.3° for the gas phase and CASPT2 calculations with the same basis set suggest a barrier of height 12.93 kJ/mol located at 0° twist angle, whereas the barrier is 6.40 kJ/mol at a 90° twist angle.[16] HF/6-31G** calculations by Tsuzuki and Tanabe[17] also obtain similar results. Calculations with MP2, MP3, and MP4(SDQ) in electron correlations using the 6-31G* basis set suggest that the effect of electron correlations on the barrier heights is not large.

Biphenyl, substituted biphenyls and other polyphenyls exhibit phase transitions driven by the change in the dihedral angle between the phenyl rings due to changes in external conditions. The flattening of the two phenyl rings causes greater overlap of the π electrons and this leads to a redshift of both the electronic transitions[18] and some of the vibrational modes.[19]

Almost all of the above studies investigate behavior of biphenyl with temperature. Only, a few studies focus on properties of biphenyl as a function of pressure. Kato et al.[20] have studied the changes in the dihedral angle of biphenyl in CS_2 as a function of pressure between 0 and 1.4 GPa. They observed a change in dihedral angle from 45° to 20°. Changes in optical and electronic properties of biphenyl as well as higher polyphenyls due to increase in pressure have been studied by Raman scattering measurements[13−15,21] and IR spectroscopy.[22,23] The disappearance of specific IR peaks has been used to characterize the decrease in the dihedral angle between the two phenyl rings.

In this work, we study the pressure dependence of the properties at room temperature in the solid phase of biphenyl. We have employed variable shape simulation cell Monte Carlo calculations in the isothermal−isobaric ensemble. Properties such as molecular conformation, radial distribution functions, lattice parameters, and volume are reported. Shifts in the frequency of certain vibrational modes have been computed from the Gaussian 98 package.[24] These results are in good agreement with IR studies of Zhuravlev and McCluskey[22,23] on biphenyl and Raman measurements of polyphenyls by Guha et al.[13−14,21]

2. Methods

2.1. Intermolecular Potential. There are several potentials proposed for hydrocarbons in the literature. Here, we have used potential parameters proposed by Williams and Cox.[25] This has been derived by fitting to about 30 aromatic and nonaromatic hydrocarbons. There are 22 sites per biphenyl molecule, one on each of the carbon and hydrogen atoms. The site−site

* To whom correspondence should be addressed.

10.1021/jp037484g CCC: $27.50
Published on Web 03/04/2004

interaction is of the Buckingham 6-exp form with an additional Coulombic term:

$$u_{ij} = b_{ij} \exp(-r_{ij}c_{ij}) - a_{ij}/r_{ij}^{\ 6} + q_i q_j / r_{ij} \qquad (1)$$

The Williams potential places a charge of $+q$ ($q = 0.153\ |e|$) on each hydrogen and a charge of $-q$ on each carbon. Potential parameters are listed in Table 1.

2.2. Intramolecular Potential. It is well-known that the intramolecular potential of biphenyl consists of two parts. The steric interaction of the atoms at the ortho positions modeled in terms of nonbonded interactions between hydrogens and carbons of the two rings at the ortho position is the first part. The second is the conjugation energy.[26] Several models have been proposed for the former. Of the available potentials, the oldest is that by Bartell.[27] Most potentials include only the H−H nonbonded interaction, but as Bartell has pointed out, the C−H and C−C interactions also play an important role. Apart from the C−C, C−H interactions, the overall barrier for the planar conformation plays a major role. Bartell's potential, which accounts for these factors, yields a barrier height of 21.8 kJ/mol across $\theta = 0°$ which is rather large. π electron calculations without geometry optimization have yielded a higher barrier height across the planar conformation (20 kJ/mol) than across the perpendicular conformation (8.4 kJ/mol). Barrier heights for the Bartell potential are close to the values obtained from this calculation. More accurate ab initio calculations incorporating geometry optimization specially for the inter-ring C−C bond suggests that the barrier heights are in fact 5.0 and 18.8 kJ/mol for the planar and perpendicular forms. Bartell's potential has been used earlier to predict the properties of solid and gaseous biphenyl. The potential due to Haigh[26] models the nonbonded interaction potential in terms of the H−H interaction term alone. Here we have chosen Benkert, Heine, and Simmons (BHS)[28] potential for modeling the torsional degrees of freedom. This intramolecular potential has the following form:

$$V(\theta) = g(L \exp[-N(\theta^2) + M \sin^2(\theta)]) \qquad (2)$$

where θ is the dihedral angle in radians. Potentials by Bartell[27] and by Haigh[26] take into consideration only the nonbonded interactions i.e., the steric interaction between the atoms at the ortho positions. In contrast, the BHS potential includes the conjugation energy in addition to the steric interaction. Further, the BHS potential appears to predict the properties correctly[29] due to inclusion of steric repulsion. The intramolecular potential parameters are listed in Table 1.

2.3. Variable Shape NPT-MC Simulations. All simulations were carried out employing the Metropolis Monte Carlo method within the isothermal−isobaric ensemble.[30,31] Here the average of any property a is given by

$$\langle a \rangle = \frac{\int \mathrm{d}V \int \mathrm{d}\Omega^N \int \mathrm{d}\theta^N \int \mathrm{d}\boldsymbol{r}^N a(\boldsymbol{r}^N,\Omega^N,\theta^N) p(\boldsymbol{r}^N,\Omega^N,\theta^N)}{\int \mathrm{d}V \int \mathrm{d}\Omega^N \int \mathrm{d}\theta^N \int \mathrm{d}\boldsymbol{r}^N \mathrm{p}(\boldsymbol{r}^N,\Omega^N,\theta^N)} \qquad (3)$$

where $p(\boldsymbol{r}^N,\Omega^N,\theta^N) = \mathrm{e}^{-\beta \mathrm{U}(\mathbf{r}^N,\Omega^N,\theta^N)}$ and $a(\boldsymbol{r}^N,\Omega^N,\theta^N)$ are the probability and the property for each configuration $(\boldsymbol{r}^N,\Omega^N,\theta^N)$. $\boldsymbol{r}^N$ are the center of mass positions of the molecules and Ω^N specify the orientations of molecules as a whole, whereas θ^N specify the dihedral angles of the N molecular species. Note that $\boldsymbol{r}$ and Ω are vectors with three components each. $\boldsymbol{r}$ specifies the three Cartesian coordinates and Ω is the three Euler angles. In contrast, θ is a scalar and refers to the value of the dihedral angle.

TABLE 1: Intermolecular and Intramolecular Potential Parameters for Biphenyl

Williams potential			
type	b_{ij}, kJ/mol	c_{ij}, Å^{-1}	a_{ij}, kJ/mol Å^6
C−C	369743.0	3.60	2439.8
C−H	66529.6	3.67	576.8
H−H	11971.0	3.74	136.4
BHS potential			
g	L, kJ/mol	M, kJ/mol	N, rad^{-2}
2	35.2	41.05	2.52

Variable shape simulation cell was employed as it provides the necessary degrees of freedom for the simulation cell to be in any one of the crystal systems. In this simulation, the simulation cell of volume V is represented by three vectors, the cell vectors, **a**, **b**, and **c**. Parrinello and Rahman[30] originally chose the three vectors without any constraints. The cell vectors have nine additional degrees of freedom. This is in addition to the $3N$ for the center of mass positions, $3N$ for the three molecular orientations and N degrees of freedom for the dihedral angle giving a total, in all, of $7N + 9$. However, as Yashonath and Rao[31] showed subsequently, only 6 degrees of freedom are necessary for representing the simulation cell. These could be, for example, the typical cell parameters a,b,c and α,β,γ. The three additional degrees of freedom in the original formulation of Parrinello and Rahman often leads to rotation of the simulation cell[31] as a whole. This can be overcome by reducing the 9 degrees of freedom to the essential 6. This has been done here by choosing vector **a** along x axis, **b** in xy plane, and **c** in any direction. This leads to a total of 6 degrees of freedom. This permits the system to undergo solid−solid phase transformation from one space group to another. Thus, the simulation has $(7N + 6)$ degrees of freedom. In systems like biphenyl the amplitude of the torsional mode involving the torsional displacement of the two phenyl rings is comparable to the molecular translation or rotation modes. Hence, it is necessary to sample over the torsional degrees of freedom in the configurational phase space to reproduce the experimentally observed structural quantities.

2.4. Ab Initio Calculations. Calculations on a single molecule of biphenyl have been carried out using Gaussian 98 to obtain the vibrational spectra. Density functional calculations (DFT) using Becke 3-parameter method and Lee−Yang−Parr electron correlation functional were carried out with 6-31G(d) basis for different values of the dihedral angle (the angle between the two phenyl rings). The dihedral angle for the ab initio calculations were those obtained from the NPT-MC variable shape simulations at various pressures. The calculation of the vibrational spectra have been carried out with no constraints on the molecular geometry except for the dihedral angle which was fixed at the average value given by the MC simulation. Vibrational frequencies and their corresponding intensities have been calculated.

2.5. Computational Details. All simulations have been carried out with 144 molecules in $4 \times 6 \times 3$ crystallographic unit cells of biphenyl consisting of a total of 3168 interaction sites. The starting configuration is the crystallographic positions reported by Trotter[1] at 300 K.

In these sets of simulations, each Monte Carlo step consists of a random translational displacement of the center of mass (com), a random rotational displacement around a randomly chosen axis and a random intramolecular rotation around the central C−C bond joining the two rings. More details of the way the method is implemented can be had from ref 31. The

TABLE 2: $\langle U_{inter} \rangle$ and Cell Parameters for Biphenyl as a Function of Pressure at 300 K

P, GPa	$\langle U_{inter} \rangle$, kJ/mol	*a*, Å	*b*, Å	*c*, Å	α, deg	*β*, deg	*γ*, deg
0.0001	−82.05	8.68	5.46	9.78	89.98	96.17	89.97
0.5000	−86.67	8.46	5.36	9.48	90.16	93.48	90.04
0.7000	−87.40	8.35	5.34	9.42	90.10	92.83	90.05
0.8000	−87.40	8.30	5.34	9.40	90.00	92.74	90.01
0.9000	−87.65	8.24	5.33	9.39	90.22	92.68	90.03
1.0000	−87.58	8.23	5.31	9.36	90.00	92.40	89.98
1.2000	−87.14	8.14	5.31	9.35	90.21	92.36	90.09
1.4000	−86.72	8.06	5.31	9.31	90.23	92.01	90.08
1.6000	−86.07	7.99	5.30	9.30	90.08	92.05	90.02
1.8000	−85.19	7.93	5.30	9.30	90.16	91.96	90.07
2.0000	−84.02	7.87	5.29	9.28	90.15	91.96	90.09
2.5000	−80.87	7.75	5.28	9.26	90.11	91.91	90.06
3.0000	−77.32	7.66	5.27	9.24	90.21	91.73	90.09
3.5000	−73.24	7.56	5.27	9.21	90.12	91.44	90.08
4.0000	−68.96	7.50	5.26	9.19	90.06	91.20	90.03
0.0001[a]		8.12	5.64	9.47	90.00	95.40	90.00
0.0001[b]		7.82	5.58	9.44	90.00	94.62	90.00

[a] Experimental at 300 K[1]. [b] Experimental at 110 K[3].

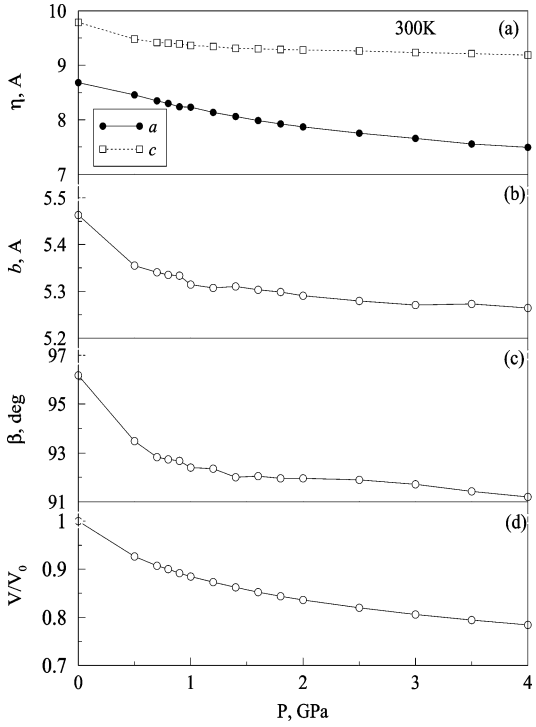

Figure 1. Variation of lattice parameters (denoted by η) with pressure (1atm to 4 GPa) for room temperature (300 K) biphenyl. (a) cell parameters *a* and *c*, (b) *b*, (c) β, and (d) V/V_0.

way temperature and pressure appears in the calculation are through the Boltzmann probabilities in eq 3. After these Monte Carlo attempts on all of the biphenyl molecules, three displacement moves on the three cell parameters are attempted. The acceptance ratio for MC moves is kept around 0.4 to ensure that the sampling over the configurational phase space is efficient. All simulations were carried out at a constant temperature of 300 K. Simulations have been carried out at different pressures of 1 atm (0.1 MPa), 0.5, 0.7, 0.8, 0.9, 1.0, 1.2, 1.4, 1.6, 1.8, 2.0, 2.5, 3.0, 3.5, and 4.0 GPa. The initial configuration for each pressure is the final configuration from the previous lower pressure simulation except for the simulation at 1 atmospheric pressure where the initial configuration is that taken from experimental crystallographic structure. Each simulation involves a total of 10 000 MC steps including 4000 for equilibration. In all of these simulations a com−com cutoff of 12.5 Å has been employed. In these systems (like many other

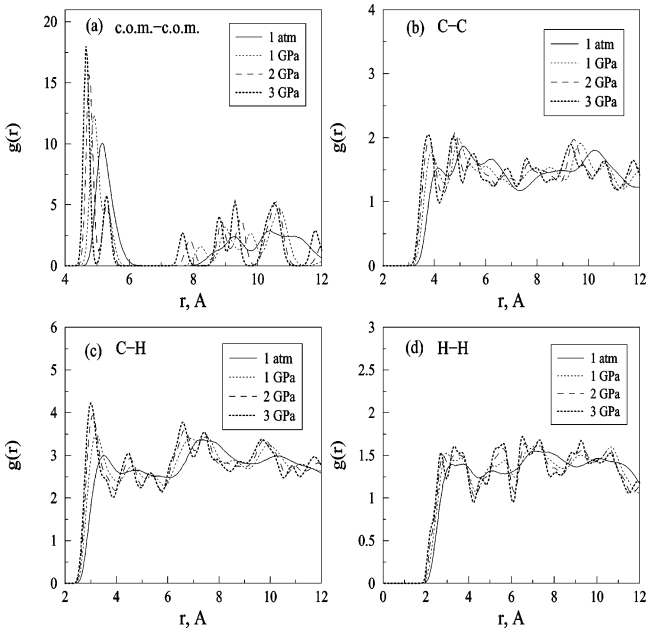

Figure 2. com−com, C−C, C−H, and H−H radial distribution functions at 300 K and at various pressures of 1 atm and 1, 2, and 3 GPa.

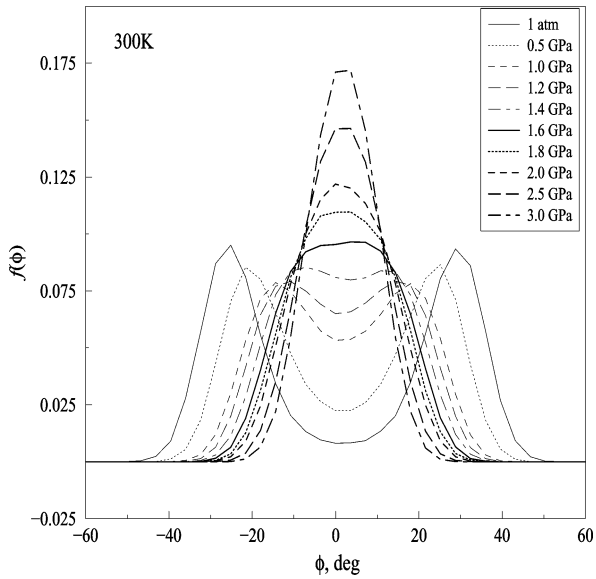

Figure 3. Dihedral angle (angle between the two phenyl rings in biphenyl) distributions at 300 K and at various pressures from 1 atm to 3 GPa.

organic molecular systems), the Coulombic contribution is less than 2% to the total intermolecular energy,[29] and hence, it was found adequate to carry out direct summation of the Coulombic terms in real space with com-com cutoff to avoid nonconvergence arising from the calculation of energy in nonneutral spheres.

3. Results and Discussions

3.1. Structure and Energetics. Radial distribution functions, lattice parameter variations with pressure, as well as different energetic contributions to the total energy of the lattice have been computed. The intermolecular energy, U_{inter}, is defined as the

$$U_{inter} = \frac{1}{2N} \sum_{a=1}^{N} \sum_{b=1}^{N} \sum_{i=1}^{N_s} \sum_{J=1}^{N_s} u_{ij} \qquad (4)$$

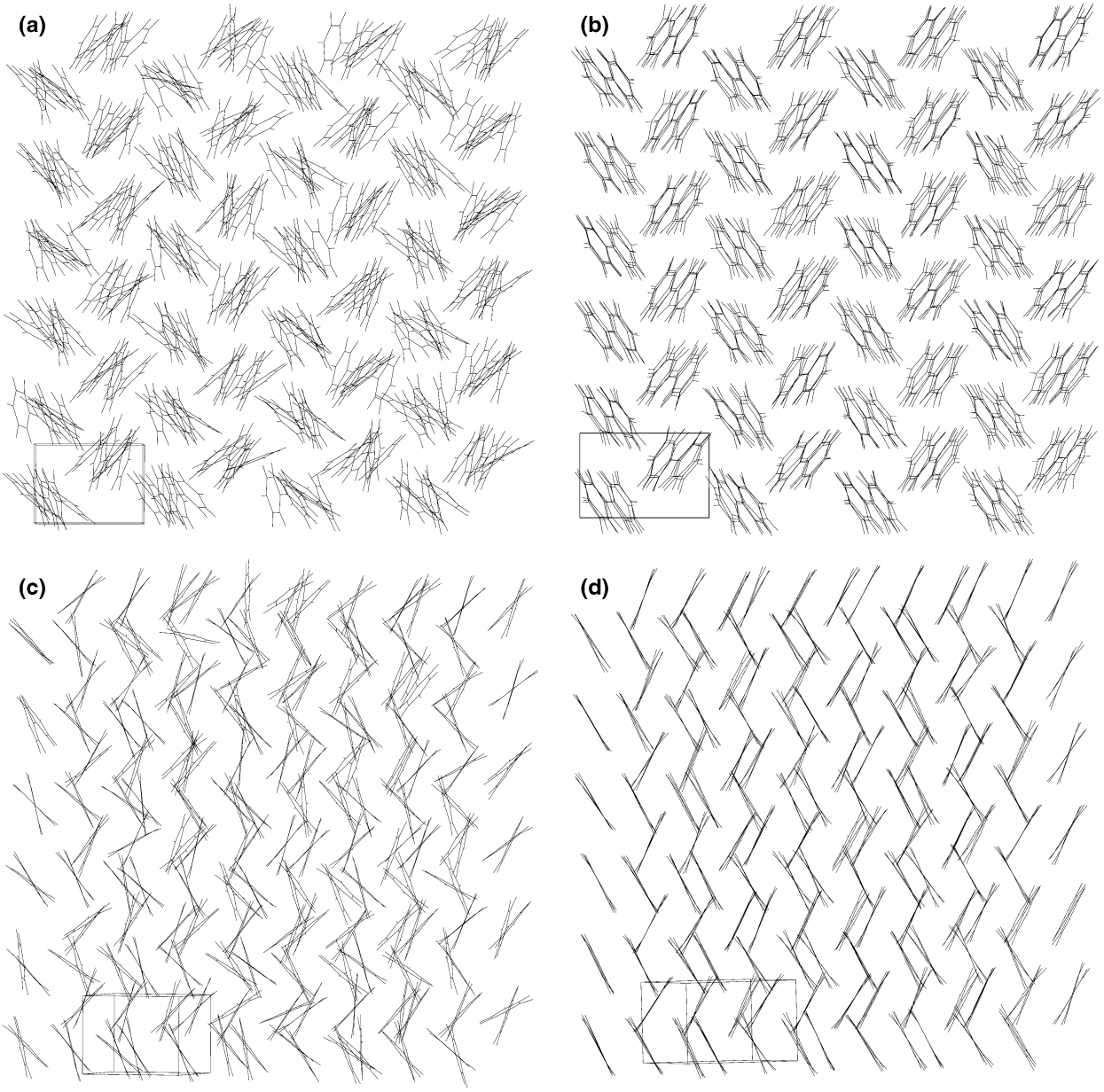

Figure 4. (a) Viewing along *c* axis (at 0.0001 GPa (1 atm)). (b) Viewing along *c* axis (at 4 GPa). (c) Viewing along molecular axis (at 0.0001 GPa). (d) Viewing along molecular axis (at 4 GPa).

where *a* and *b* refer to the molecules and *i* and *j* refer to the interaction sites placed at the positions of C and H. u_{ij} is given by the expression in eq 1 and consists of both short range and Coulomb interactions. The intramolecular energy U_{intra} and U_{total} are given by

$$U_{\text{intra}} = \frac{1}{N}\sum_{i=1}^{N} V(\theta) \tag{5}$$

$$U_{\text{total}} = U_{\text{inter}} + U_{\text{intra}} \tag{6}$$

Lattice parameters and $\langle U_{\text{inter}} \rangle$ at different pressures obtained from NPT Monte Carlo simulation of biphenyl are listed in Table 2 along with experimental data where available. The values of *a* and *c* at 300 K are slightly higher, whereas that of *b* is lower than found from experiment at $P = 1$ atm and $T =$ 300 K. Angle β is somewhat larger (96.17°) than the experimental value (95.40°). Variation of some of the lattice parameters with pressure are plotted in Figure 1. We found that the first derivative of the lattice parameters and volume did show discontinuities with pressure indicating that biphenyl might undergo a phase transition around 0.8 GPa. The transition probably is of second order.[32]

Figure 2 shows a plot of the com-com, C−C, C−H and H−H radial distribution functions (rdf) at four different pressures at 300 K. The rdf at 1 atm pressure show little structure. In contrast, the rdf at higher pressures show significant structure. Even at the relatively low pressure of 1 GPa significant structure is seen. Appearance of well-defined features in the rdf generally suggests a transition from a disordered structure to an ordered structure. For example, plastic crystal to crystalline transition seen in globular molecules such as methane, neopentane, etc., shows well-defined features or peaks in the rdf near the temperature at which the transition from the orientationally disordered to ordered phase takes place.[33] In the case of biphenyl, the disorder is of the dihedral angle. The width of the peaks in the center of mass rdf narrows with increase in pressure which suggests better

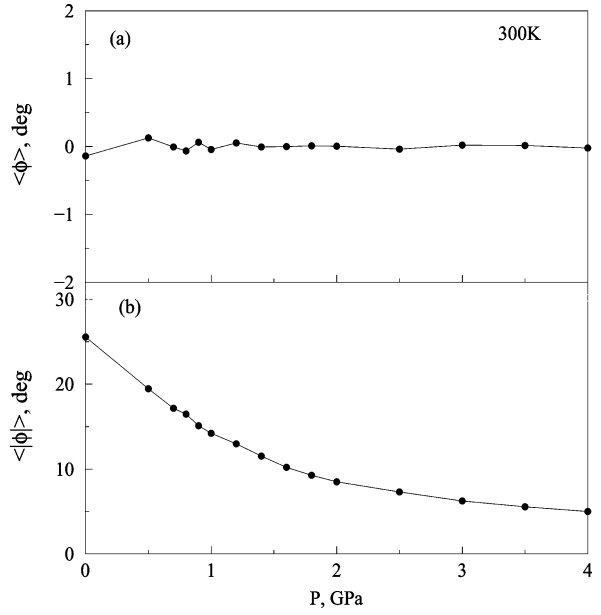

Figure 5. Variation of average dihedral angle and average absolute dihedral angle and its derivative: (a) average dihedral angle; (b) average absolute dihedral angle.

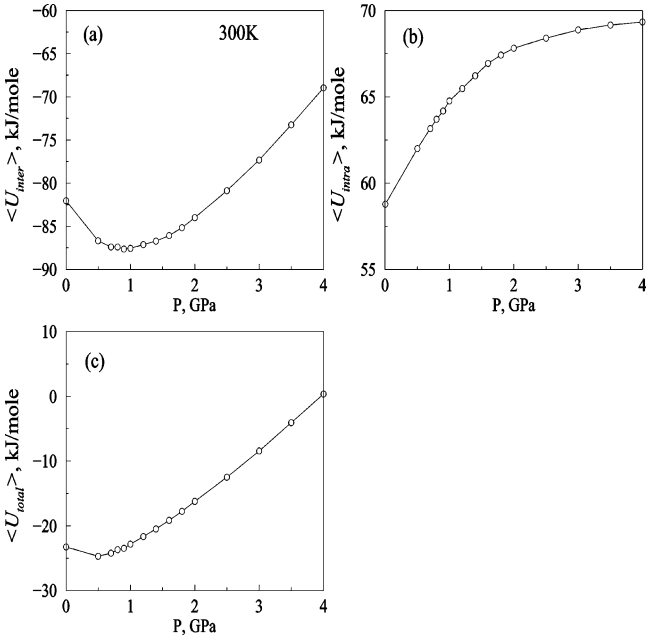

Figure 6. Variation of inter and intramolecular interactions with pressure in the range 1 atm to 4 GPa at 300 K. (a) $\langle U_{\text{inter}}\rangle$, (b) $\langle U_{\text{intra}}\rangle$, and (c) $\langle U_{\text{total}}\rangle$.

packing with increase in pressure which as we shall see also leads to a decrease in U_{inter} with increase in pressure.

To understand the nature of the order, we show a plot of the distribution of the dihedral angle at various pressures (Figure 3). Note the bimodal distribution[7] with maxima at dihedral angles of $\phi = \pm 30°$. In agreement with our previous study on biphenyl,[28] the present calculations also suggest that the biphenyl room temperature phase has a dynamically disordered distribution of dihedral angles. Each biphenyl is frequently undergoing transition from one minima to another of a bistable or double well potential. There is sufficient evidence in the literature for this. For example, the triplet-state electron nuclear double resonance (ENDOR) results of Brenner et al.,[8] directly show the loss of the center of symmetry in the room-temperature structure of biphenyl.

The distribution at 0.5 GPa is similar, but by 1.0 GPa, the bimodal distribution has nearly transformed to an unimodal distribution. The energy barrier ϵ_{wd} from $\phi = +30°$ to $\phi = -30°$ is now less than $k_{\text{B}}T$, and therefore, there are frequent transitions from one minima to another.

At pressures lower than 1 GPa, the most probable value of the dihedral angle is around 30°, whereas the average value is close to zero. This is also evident from Figure 4, parts a and b showing a snapshot view of biphenyl crystal structure at 300 K and 1 atm as well as 4 GPa, respectively. The view is looking down the *c* axis of the monoclinic simulation cell (space group $P2_1/a$).[1] The nonplanar nature of the biphenyl and consequent disorder in the two phenyl rings of different biphenyl at 1 atm is evident. At 4 GPa, an increased ordering can be seen clearly. Also shown is a view down the long molecular axis (see Figure 4, parts c and d). In this view, one can see more clearly the different dihedral angles of various biphenyl molecules at 1 atm. The scissor-like structure of each of the biphenyl shows that the molecules have a dihedral angle different from zero. In contrast, the single line and a significant reduction in the scissor-like structures at 4 GPa suggests the onset of ordering and flattening of the molecules. The dynamical disorder is responsible for the absence of well-defined features in the C−C, C−H, and H−H rdf while the com-com, rdf is unaffected by this disorder. This, however, is not the case at pressures equal to and above 1.0 GPa. With an increase in pressure, the biphenyls actually approach a unimodal distribution with the most probable distribution coinciding with the average value of the distribution.

Figure 5 shows a plot of the average of dihedral angle, average of the modulus of the dihedral angle. The derivative of the absolute value of the dihedral angle with pressure also showed a discontinuity at around the same pressure as the lattice parameters.

We now analyze the competing interactions at the molecular level to understand the microscopic nature of this transition. A variation of $\langle U_{\text{inter}}\rangle$, $\langle U_{\text{intra}}\rangle$, and $\langle U_{\text{total}}\rangle$ with pressure are shown in Figure 6. $\langle U_{\text{inter}}\rangle$ shows a minimum near 0.8 GPa. In contrast, $\langle U_{\text{intra}}\rangle$ shows a monotonic increase with pressure. The behavior of $\langle U_{\text{total}}\rangle$ is determined by the larger of these two terms, viz., $\langle U_{\text{inter}}\rangle$. $\langle U_{\text{inter}}\rangle$ shows a minimum in the range 0.5−1 GPa. Typically, one expects the total as well as all other energy terms of intermolecular interactions to increase with increase in pressure. This is true of U_{intra} but not of U_{inter} (and therefore U_{total}). This strange situation arises because of the flattening of the biphenyl leads to better crystal packing which in turn leads to a *decrease* in U_{inter}. Similar behavior may be expected of other phenyls such as terphenyl, tetraphenyl, or hexaphenyls, etc. The behavior of $\langle U_{\text{total}}\rangle$ as well as the unit cell volume with pressure is also reflected in the calculated specific heat and compressibility shown in Figures 7 and 8.

$$C_{\text{p}} = \frac{\langle H^2\rangle - \langle H\rangle^2}{k_{\text{B}}T^2} \tag{7}$$

$$\kappa = \frac{\langle V^2\rangle - \langle V\rangle^2}{\langle V\rangle k_{\text{B}}T} \tag{8}$$

Here H is the enthalpy and given by $H = U_{\text{total}} + PV$ where P is the pressure and V the volume. Specific heat shows clear evidence of the transition near 0.8 GPa.

From the simulation, the variation of the total intermolecular interaction energy of a given molecule (averaged over the whole ensemble) with ϕ can be obtained. Figure 9 shows the variation

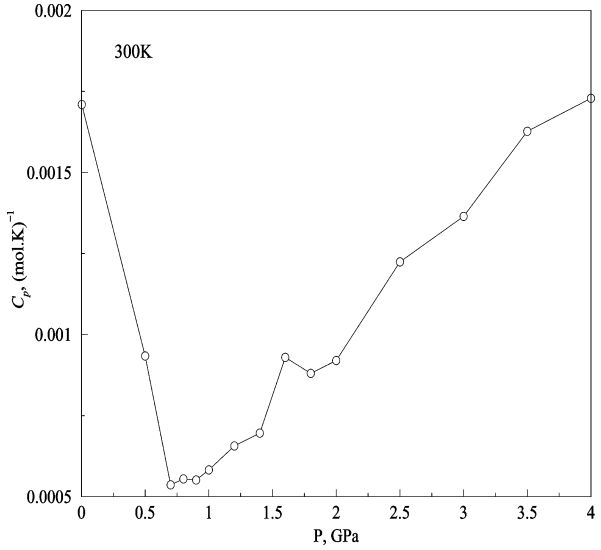

Figure 7. Pressure dependence of constant pressure specific heat, C_p.

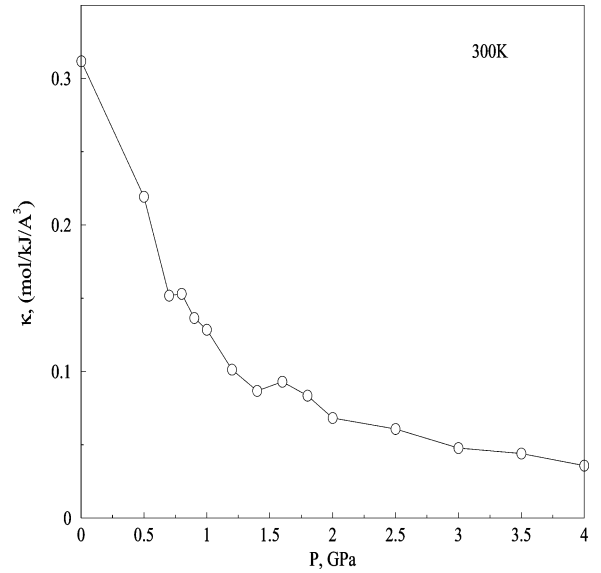

Figure 8. Pressure dependence of compressibility κ.

of $\langle U_{\text{total}} \rangle$ as a function of ϕ, the dihedral angle at different pressures. The double well potential at low pressures gradually changes to a single well potential. This is consistent with the distribution of the dihedral angle with pressure seen in Figure 3. We note that increasing pressure leads to planarity of the two rings just the way increasing the temperature also leads to planarity of the two rings. However, the changes in $U_{\text{total}}(\phi)$ seen here are quite different from the changes seen when the temperature is increased. On increasing the temperature, contribution of $\langle U_{\text{inter}} \rangle$ *decreases*, whereas with an increase in pressure, it *increases*. The barrier for rotation around the long axis of the molecule, ϵ_{wd} (equals the difference in U_{total} at $\phi = 0$ and the minimum value of U_{total}), shows no decrease when the temperature is increased. However, the large kinetic energy at higher temperatures leads to frequent transition from one minima to another. The value of ϵ_{wd} at 1 atm is seen to be nearly 8 kJ/mol. This may be compared with $\Delta E_{\text{np}\rightarrow\text{p}} = 0.089$ eV (or 8.59 kJ/mol), the difference in internal energy between the nonplanar (np) and planar (p) conformation obtained from density functional calculations by Guha et al.[13]

In contrast to this, on increasing the pressure, this barrier is reduced gradually until there is none. The contribution of U_{inter}

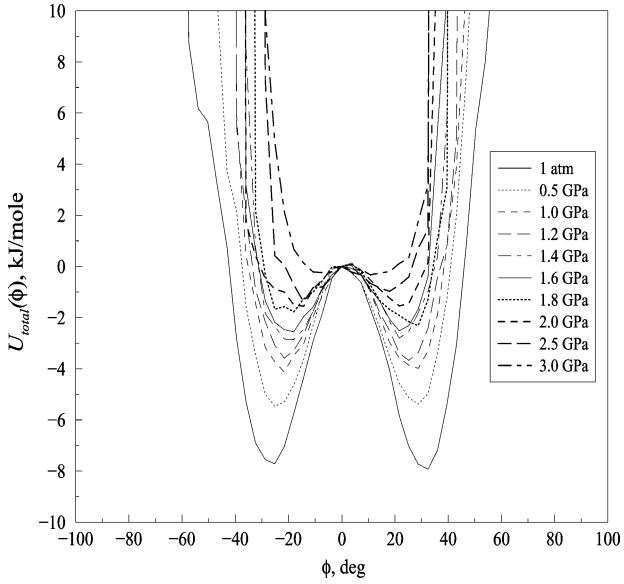

Figure 9. $U_{\text{total}}(\phi)$ distribution as a function of dihedral angle at 300 K and at various pressures from 1 atm to 3 GPa.

in this is significant and is the larger of the two. Unlike U_{intra} which shows a monotonic increase, U_{inter} exhibits a minimum around 0.8 or 0.9 GPa. This value of pressure in consistent with the discontinuity in the first derivative of several properties such as lattice parameters, a, b, c, β and volume and absolute value of the dihedral angle. Such a discontinuity is also seen in the variation of the IR intensity at 714.7 and 796.9 cm^{-1} around 0.8 GPa. Unfortunately, the MC simulations have not been performed at uniform spacing of pressure, and therefore, these are not shown. Signatures of this are also seen in C_p and κ as a minimum and discontinuity respectively (see Figures 7 and 8).

3.2. Vibrational Spectra. Recently, Rumi and Zerbi,[34] Furuya et al.,[35] and Zhuravlev and McCluskey[22] have reported ab initio calculations on biphenyl. Following these, density functional calculations employing Becke 3-parameter method and Lee−Yang−Parr electron correlation functional were carried out using the Gaussian 98 package.[24] The basis set used was 6-31G(d). Calculations were performed on a single biphenyl for the dihedral angles obtained from the variable shape NPT-MC simulation. Zhuravlev and McCluskey[22,23] have looked at the changes in the IR spectra of biphenyl due to hydrostatic pressure up to 2 GPa at liquid helium temperatures. They carried out experiments using a diamond anvil cell and used ab initio calculations to assign the experimentally observed frequencies. Of the several frequencies they have studied, two have been looked at in detail by them. These are the H out-of-plane bending modes at frequencies 714.7 and 796.9 cm^{-1}. These two have a symmetry B_3 and are IR active when the biphenyl molecule is in a nonplanar or twisted conformation ($\phi \neq 0$). We have also followed the intensity of transition of these two vibrational modes as a function of the dihedral angle using the Gaussian 98 package. As the dihedral angle approaches zero, these two modes become IR inactive. Intensity variation of these two modes with increase in hydrostatic pressure due to increasing planarity as obtained from the vibrational analysis is shown in Figure 10. A significant decrease in intensity is seen to occur by about 0.8 GPa. Beyond this pressure, the intensity reduces slowly and could vanish eventually. This may be compared with the disappearance of vibrational peaks between 0.07 and 0.45 GPa by Zhuravlev and McCluskey[22,23] at liquid-helium temperatures. Their study points to the existence

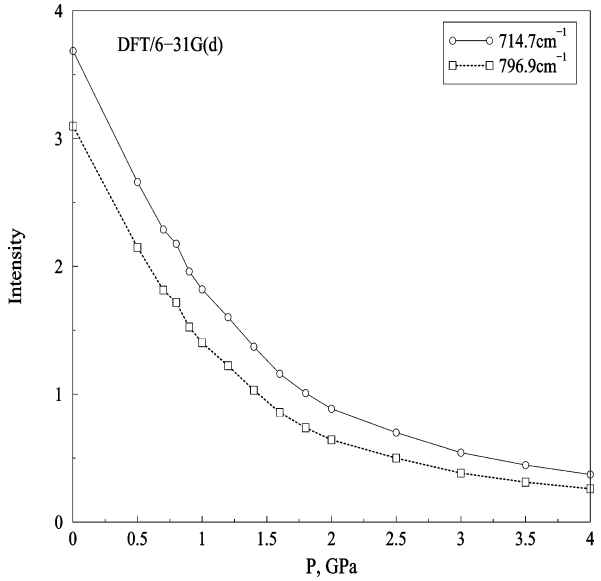

Figure 10. IR intensity as a function of pressure for the modes (out-of-plane bending modes of hydrogen atoms) corresponding to the frequencies of 714.7 and 796.9 cm^{-1}.

of a phase transition due to a transition from twisted to planar conformation. Present calculations are at 300 K, and at these higher temperatures, it is reasonable to expect that the transition pressure will be higher due to increased entropy associated with higher disorder in the dihedral angle.

3.3. Conclusions. The present calculation shows that with an increase in pressure the room temperature solid phase of biphenyl undergoes a transition to another phase. The transition is associated with the dihedral angle becoming zero. The increased symmetry of the molecular geometry of planar biphenyl leads to better crystal packing of the molecules. Initially this leads to lowering of U_{inter}. At around 0.8 GPa, U_{inter} reaches a minimum, but beyond this pressure, U_{inter} gradually increases. However, biphenyl remains planar, and the increase in U_{inter} is purely due to larger contribution from the repulsive interactions. The amplitude of the torsional motion decreases significantly with increase in pressure up to 0.8 GPa, but beyond, this it decreases only marginally. There appears to be a phase transformation at around 0.8 GPa to another phase where biphenyls are all planar. Vibrational modes at 714.7 and 796.9 cm^{-1} show a decrease in intensity with the flattening of biphenyl. Derivative of lattice parameters, volume, the absolute value of the dihedral angle, and the IR intensity of the peaks all show discontinuity at 0.8 GPa suggesting a possible transition at this pressure.

Acknowledgment. Authors (N.A.M. and S.Y.) wish to thank Department of Science & Technology, New Delhi for financial support.

References and Notes

(1) Trotter, J. *Acta Crystallogr.* **1961**, *14*, 1135.
(2) Cailleau, H.; Baudour, J. L.; Zeyen, C. M. *Acta Crystallogr. B* **1979**, *35*, 426.
(3) Almenningen, A.; Bastiansen, O.; Fernholt. L.; Cyvin, B. N.; Cyvin, S. J.; Samdal, S. J. *J. Mol. Struct.* **1985**, *128*, 59.
(4) Bastiansen, O.; Samdal, S. *J. Mol. Struct.* **1985**, *128*, 115.
(5) Tinland, B. *J. Mol. Struct.* **1969**, *3*, 161.
(6) Suzuki, H. *Bull. Chem. Soc. Jpn.* **1959**, *32*, 1340.
(7) Ponte Goncalves, A. M. *Prog. Solid State Chem.* **1980**, *13*, 1.
(8) Brenner, H. C.; Hutchison, C. A., Jr.; Kemple, M. D. *J. Chem. Phys.* **1974**, *60*, 2180.
(9) Hochstrasser, R. M.; McAlpine, R. D.; Whiteman, J. D. *J. Chem. Phys.* **1973**, *58*, 1078.
(10) Launois, P.; Moussa, F.; Lemee-Cailleau, M. H.; Cailleau, H. *Phys. Rev. B* **1989**, *40*, 5042.
(11) Ecolivet, C.; Sanquer, M.; Pellegrin, J.; De Witte, J. *J. Chem. Phys.* **1983**, *78*, 6317.
(12) Barich, D. H.; Pugmire, J. R.; Grant, D. M.; Iuliucci, R. J. *J. Phys. Chem. A* **2001**, *105*, 6780.
(13) Guha, S.; Graupner, W.; Resel, R.; Chandrasekhar, M.; Chandrasekhar, H. R.; Glaser, R.; Leising. G. *Phys. Rev. Lett.* **1999**, *82*, 3625.
(14) Graupner, W.; Resel, R.; Leising, R.; Glaser, R.; Guha, S.; Chandrasekhar, M.; Chandrasekhar, H. R. *Synth. Met.* **1999**, *101*, 180.
(15) Lemee-Cailleau, M. H.; Girard, A.; Cailleau, H.; Delugeard, Y. *Phys. Rev. B* **1992**, *45*, 12682.
(16) Rubio, M.; Merchan, M.; Orti, E. *Theor. Chim. Acta* **1995**, *91*, 17.
(17) Tsuzuki, S.; Uchimura, T.; Matsumura, K.; Mikami, M.; Tanabe, K. *J. Chem. Phys.* **1999**, *110*, 2858.
(18) Ramasesha, S.; Albert, I. D. L.; Sinha, B. *Mol. Phys.* **1991**, *72*, 537.
(19) Pusching, P.; Ambrosch-Draxl, C.; Heimel, G.; Zojer, E.; Resel, R.; Leising, M.; Kriechbaum, M.; Graupner, W. *Synth. Met.* **2001**, *116*, 327.
(20) Kato, M.; Higashi, M.; Taniguchi, Y. *J. Chem. Phys.* **1988**, *89*, 5417.
(21) Guha, S.; Graupner, W.; Resel, R.; Chandrasekhar, M.; Chandrasekhar, H. R.; Glaser, R.; Leising. G. *J. Phys. Chem. A* **2001**, *105*, 6203.
(22) Zhuravlev, K. K.; McCluskey, M. D. *J. Chem. Phys.* **2002**, *117*, 3748.
(23) Zhuravlev, K. K.; McCluskey, M. D. *J. Chem. Phys.* **2001**, *114*, 5465.
(24) Frisch, M. J.; Trucks, G. W.; Schlegel, H. B.; Scuseria, G. E.; Robb, M. A.; Cheeseman, J. R.; Zakrzewski, V. G.; Montgomery, J. A., Jr.; Stratmann, R. E.; Burant, J. C.; Dapprich, S.; Millam, J. M.; Daniels, A. D.; Kudin, K. N.; Strain, M. C.; Farkas, O.; Tomasi, J.; Barone, V.; Cossi, M.; Cammi, R.; Mennucci, B.; Pomelli, C.; Adamo, C.; Clifford, S.; Ochterski, J.; Petersson, G. A.; Ayala, P. Y.; Cui, Q.; Morokuma, K.; Malick, D. K.; Rabuck, A. D.; Raghavachari, K.; Foresman, J. B.; Cioslowski, J.; Ortiz, J. V.; Stefanov, B. B.; Liu, G.; Liashenko, A.; Piskorz, P.; Komaromi, I.; Gomperts, R.; Martin, R. L.; Fox, D. J.; Keith, T.; Al-Laham, M. A.; Peng, C. Y.; Nanayakkara, A.; Gonzalez, C.; Challacombe, M.; Gill, P. M. W.; Johnson, B. G.; Chen, W.; Wong, M. W.; Andres, J. L.; Head-Gordon, M.; Replogle, E. S.; Pople, J. A. *Gaussian 98*, revision A.9; Gaussian, Inc.: Pittsburgh, PA, 1998.
(25) Williams, D. E.; Cox, S. R. *Acta Crystallogr. B* **1984**, *40*, 404.
(26) Fisher-Hjalmars, I. *Tetrahedron.* **1963**, *19*, 1805.
(27) Bartell, L. S. *J. Chem. Phys.* **1964**, *41*, 3928.
(28) Benkert, C.; Heine, V.; Simmons, E. H. *J. Phys. Chem.* **1987**, *20*, 3337.
(29) Chakrabarti, A.; Yashonath, S.; Rao, C. N. R. *Mol. Phys.* **1995**, *84*, 49.
(30) Parrinello, M.; Rahman, A. *Phys. Rev. Lett.* **1980**, *45*, 1196.
(31) Yashonath, S.; Rao, C. N. R. *Chem. Phys. Lett.* **1985**, *119*, 22.
(32) Rao, C. N. R.; Rao, K. J. *Phase transitions in solids*; McGraw Hill International: New York, 1978.
(33) Sherwood, J. N. *Plastically crystalline state: Orientationally disordered crystals*; Wiley: New York, 1979.
(34) Rumi, M.; Zerbi, G. *Chem. Phys.* **1999**, *242*, 123.
(35) Furuya, K.; Torii, H.; Furukawa, Y.; Tasumi, M. *J. Mol. Struct.* **1998**, *424*, 225.